

Non-dimensional parameters for the flapping dynamics of multilayered plates*

Aditya Karthik Saravanakumar, Supradeepan K., and P. S. Gurugubelli†

Computing Lab, Department of Mechanical Engineering,
Birla Institute of Technology and Science - Pilani, Hyderabad.

(Dated: April 15, 2021)

Coupled flow-induced flapping dynamics of flexible plates are governed by three non-dimensional numbers: Reynolds number, mass-ratio, and non-dimensional flexural rigidity. The traditional definition of these parameters is limited to isotropic single-layered flexible plates. There is a need to define these parameters for a more generic plate made of multiple isotropic layers placed on top of each other. In this work, we derive the non-dimensional parameters for a flexible plate of n -isotropic layers and validate the non-dimensional parameters with the aid of numerical simulations.

I. INTRODUCTION

The interaction between viscous fluid flows and flexible structures has been a popular topic of research over the past two decades. This surge in interest can be owed to a variety of phenomena that involve such coupled interactions ranging from vortex-induced vibrations [1] to biomedical applications [2]. Understanding of the underlying physical mechanisms of such coupled interactions has been enabled by investigations into simple model problems such as the flapping dynamics of a flexible plate-like structure in an external flow [3]. This particular problem has been studied in diverse contexts including energy harvesting devices [4–6], propulsion systems [7–10] and paper flutter in a printing press [11]. Energy harvesting devices are based on the piezoelectric mechanism wherein the strain energy of the flexible structure performing flapping motion is converted into electrical energy.

The earliest demonstrations [4, 12] of such energy harvesting devices were carried out by placing plate-like structures made of the piezoelectric material polyvinylidene fluoride (PVDF) in the wake of bluff bodies. Since then, studies have been conducted to optimize the energy output from such devices by studying the resonant conditions [13], flow orientation [14], plate orientation [15–18] and electrode position [19]. In these experiments, it is common for the piezoelectric materials to be mounted on thicker plate-like structures made of materials such as Mylar [13] or polyurethane [4], thereby resulting in a multilayered flexible structure for energy harvesting.

Various numerical methods based on the finite difference method [20, 21], finite element method [22, 23] and lattice Boltzmann method [24, 25], have been used to investigate the non-linear two/three-dimensional post-critical flapping response, force and vortex dynamics to understand the physics behind the flapping phenomena for isotropic flexible structures. Despite the fact that piezoelectric energy harvesting devices are multilayered, the current understanding of the non-linear

flapping dynamics is primarily limited to results from isotropic models. An attempt was made earlier by [6], who have numerically investigated the flapping dynamics of a three-layered flexible plate by considering an equivalent single-layered plate's Young's modulus for the three-layered flexible plate. More recently, in [26], a quasi-monolithic formulation to numerically investigate the post-critical flapping dynamics of a two-layered plate in a uniform flow. This study revealed that variation of material properties across the layers can result in complex flapping dynamics and there is need for the development of non-dimensional parameters that can generalize the flapping dynamics of multilayered structures.

II. CONSTRUCTION OF NON-DIMENSIONAL PARAMETERS

In this section we present an analytical derivation for the non-dimensional parameters that govern the self-sustained flapping dynamics of multilayered plates. Initially, we construct the non-dimensional parameters for a two-layered plate and then proceed to generalize the derivation for the case of a n -layered plate. The flapping dynamics of a single layered isotropic flexible plate is relatively well understood and is known to depend on the structure to fluid mass-ratio (m^*), non-dimensional flexural rigidity (K_B) and Reynolds number (Re) [21, 27, 28] which are defined as

$$m^* = \frac{\rho^s h}{\rho^f L} \quad K_B = \frac{B}{\rho^f U_0^2 L^3} \quad Re = \frac{\rho^f U_0 L}{\mu^f}, \quad (1)$$

where B and ρ^s represent the flexural rigidity and density of the flexible plate, respectively, and μ^f is the dynamic viscosity of the fluid. These definitions can be extended for multilayered flexible plates by modifying the non-dimensional parameters, i.e. m^* and K_B , to replace the single-layered plate properties such as ρ^s , h and B with their equivalent values for a multilayered plate.

Figure 1 presents a representative schematic of a two-layered flexible plate of length L and thickness h_{eq} flapping about its leading edge. The flexible plate interacts with a uniform incompressible viscous fluid of density ρ^f , flowing along its length at a flow velocity of U_0 .

* Physical Review Letters

† pardhasg@hyderabad.bits-pilani.ac.in

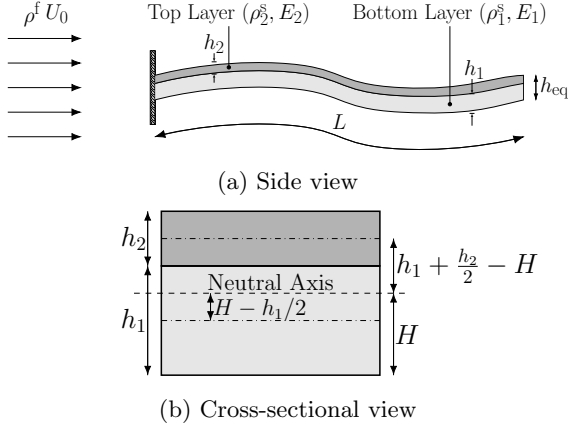


Figure 1: A schematic of a two-layered flexible plate, with a fixed leading edge, flapping in a uniform stream.

In this work, $(\rho_1^s, E_1, \nu_1, h_1)$ and $(\rho_2^s, E_2, \nu_2, h_2)$ represent the density, Young's modulus, Poisson's ratio and thickness of the bottom and top layers, respectively. The total thickness of the two-layered plate is given as $h_{eq} = h_1 + h_2$.

The structural dynamics of the flapping plate is described by the Euler-Bernoulli beam equation as

$$\rho_{eq}^s h_{eq} \frac{\partial^2 w}{\partial t^2} + B_{eq} \frac{\partial^4 w}{\partial x^4} = f, \quad (2)$$

where ρ_{eq}^s and B_{eq} represent the equivalent density and equivalent flexural rigidity for the combined two-layered plate. Here, w denotes the transverse deflection of the plate due to the fluid loading f acting on the plate. The equivalent density ρ_{eq}^s and equivalent flexural rigidity B_{eq} are defined as

$$\rho_{eq}^s = \frac{\rho_1^s h_1 + \rho_2^s h_2}{h_{eq}} \quad B_{eq} = \frac{E_1 I_1}{(1 - \nu_1^2)} + \frac{E_2 I_2}{(1 - \nu_2^2)}. \quad (3)$$

In Eq. 3, I_1 and I_2 represent the area moment of inertia for the bottom and top layers, respectively, calculated with respect to the neutral axis of the combined two-layered plate. For an isotropic plate with a uniform cross-section, the neutral axis will always pass through the centroid of the plate's cross-section. However, in the case of a two-layered or multilayered plate, the neutral axis need not pass through the centroid of the cross-section as its position depends on the thickness and Young's modulus of each layer. In such cases, the position of the neutral axis can be determined by considering the stress equilibrium condition in the stream-wise direction at any cross-section. For the case of pure bending in a two-layered plate, the equilibrium condition can be formulated as

$$\Sigma F_x = \int_A \sigma_x dA = 0 \quad (4)$$

$$-\int_0^{h_1} E_1 \frac{(y-H)}{\gamma} b dy - \int_{h_1}^{h_1+h_2} E_2 \frac{(y-H)}{\gamma} b dy = 0, \quad (5)$$

where σ_x , γ , b and H represent the normal stress along the stream-wise direction, the plate width, the radius of curvature and the distance of the neutral axis from the bottom of the plate, respectively. Equation 5 can be solved to deduce the expression for the position of a neutral axis H as

$$H = \frac{E_1 h_1 (h_1/2) + E_2 h_2 (h_1 + h_2/2)}{(E_1 h_1 + E_2 h_2)}. \quad (6)$$

The parallel axis theorem can then be used to calculate the area moments of inertia I_1 and I_2 about the neutral axis (see Fig. 1). The resulting expressions are

$$I_1 = \frac{h_1^3}{12} + h_1 \left(\frac{h_1}{2} - H \right)^2 \quad I_2 = \frac{h_2^3}{12} + h_2 \left(h_1 + \frac{h_2}{2} - H \right)^2. \quad (7)$$

Upon substituting these expressions in Eq. 3 we obtain the final form of the equation for the equivalent flexural rigidity (B_{eq}) as

$$B_{eq} = \frac{E_1}{(1 - \nu_1^2)} \left[\frac{h_1^3}{12} + h_1 \left(\frac{h_1}{2} - H \right)^2 \right] + \frac{E_2}{(1 - \nu_2^2)} \left[\frac{h_2^3}{12} + h_2 \left(h_1 + \frac{h_2}{2} - H \right)^2 \right] \quad (8)$$

Finally, the modified mass-ratio m_{eq}^* and non-dimensional flexural rigidity K_B^{eq} that govern the flapping dynamics of a two-layered flexible plate are defined as

$$m_{eq}^* = \frac{\rho_{eq}^s h_{eq}}{\rho^f L} \quad K_B^{eq} = \frac{B_{eq}}{\rho^f U_0^2 L^3}. \quad (9)$$

Furthermore, the expressions for H and B_{eq} in Eqs. 6 and 8, respectively, for the case of a two-layered plate can be generalized for a n -layered plate following the same equilibrium condition approach as

$$H = \frac{E_1 h_1 (h_1/2) + \dots + E_n h_n (h_1 + \dots + h_{n-1} + h_n/2)}{(E_1 h_1 + E_2 h_2 + \dots + E_{n-1} h_{n-1} + E_n h_n)} \quad (10)$$

$$H = \frac{\sum_{i=1}^n \left[E_i h_i \left(\sum_{j=1}^i h_j - \frac{h_i}{2} \right) \right]}{\sum_{i=1}^n E_i h_i}$$

$$B_{eq} = \frac{E_1}{(1 - \nu_1^2)} \left[\frac{h_1^3}{12} + h_1 \left(\frac{h_1}{2} - H \right)^2 \right] + \frac{E_2}{(1 - \nu_2^2)} \left[\frac{h_2^3}{12} + h_2 \left(h_1 + \frac{h_2}{2} - H \right)^2 \right] + \dots + \frac{E_n}{(1 - \nu_n^2)} \left[\frac{h_n^3}{12} + h_n \left(h_1 + \dots + h_{n-1} + \frac{h_n}{2} - H \right)^2 \right]$$

Case	$\frac{\rho_1^s}{\rho^f}$	$\frac{\rho_2^s}{\rho^f}$	m_{eq}^* $\times 10^{-1}$	$\frac{E_1}{\rho^f U_0^2 (1-\nu_1^2)}$	$\frac{E_2}{\rho^f U_0^2 (1-\nu_2^2)}$	K_B^{eq} $\times 10^{-4}$	C_d^{mean}	C_d^{max}	C_d^{rms}	C_l^{max}	C_l^{rms}
1	10.0	10.0	1.00	28560.4	775.8	4	0.118365	0.137339	0.012331	0.109690	0.077722
2	10.0	10.0	1.00	4800.0	4800.0	4	0.118272	0.136622	0.012339	0.107362	0.077629
3	10.0	10.0	1.00	27761.5	1641.8	5	0.107087	0.118141	0.007438	0.080946	0.058900
4	10.0	10.0	1.00	6000.0	6000.0	5	0.107165	0.117704	0.007489	0.080188	0.059392
5	10.0	5.0	0.75	1200.0	1200.0	1	0.116338	0.132610	0.010627	0.073763	0.052307
6	12.5	2.5	0.75	1200.0	1200.0	1	0.116337	0.132628	0.010623	0.073585	0.052306
7	7.5	2.5	0.50	1200.0	1200.0	1	0.094950	0.098030	0.002059	0.026021	0.018369
8	5.0	5.0	0.50	1200.0	1200.0	1	0.094904	0.098034	0.002048	0.026158	0.018427

Table I: Non-dimensional density and flexural rigidity of the top and bottom layers corresponding to the eight cases considered for validation of the proposed non-dimensional parameters. In each case $Re = 1000$ and $h_1 = h_2 = 0.005L$

$$B_{\text{eq}} = \sum_{i=1}^n \frac{E_i}{1-\nu_i^2} \left[\frac{h_i^3}{12} + h_i \left(\sum_{j=1}^i h_j - \frac{h_i}{2} - H \right)^2 \right] \quad (11)$$

Using these definitions, we can define the non-dimensional parameters for a n -layered plate, according to Eq. 9. It is noteworthy that although the equivalent mass ratio is the linear summation of the independent mass ratios of each layer, the equivalent non-dimensional flexural rigidity is not equal to the sum of the independent non-dimensional flexural rigidities of each layer.

III. NUMERICAL VERIFICATION

The newly proposed non-dimensional parameters were validated by conducting a series of eight numerical experiments to simulate the flapping dynamics of two-layered plates placed in a uniform stream for a $Re = 1000$. Table I provides the material properties of the eight cases, wherein the first four cases are used for validating the equivalent flexural rigidity K_B^{eq} and the latter four cases validate the equivalent mass ratio m_{eq}^* . For simplicity, the top and bottom layers of the plate are considered to be having the same thickness $h_1 = h_2 = 0.005L$. From Table I, it can be observed that cases 1 & 2 and cases 3 & 4 form two pairs of cases having identical nondimensional K_B^{eq} despite the pairs having different nondimensional elastic moduli $E_1/\rho^f U_0^2 (1-\nu_1^2)$ and $E_2/\rho^f U_0^2 (1-\nu_2^2)$. Similarly, cases 5 & 6 and cases 7 & 8 are two pairs of cases having identical nondimensional m_{eq}^* with different density ratios, i.e. ρ_1^s/ρ^f and ρ_2^s/ρ^f . The numerical methodology employed and the computational domain considered is identical to what was used in [26].

Figure 2 shows the temporal evolution of the trailing edge cross-stream displacement for the eight cases summarized in Table I. It can be seen that for the pairs of cases with identical non-dimensional parameters (m_{eq}^* and K_B^{eq}), the trailing edge cross-stream displacements perfectly overlap and possess similar flapping amplitude

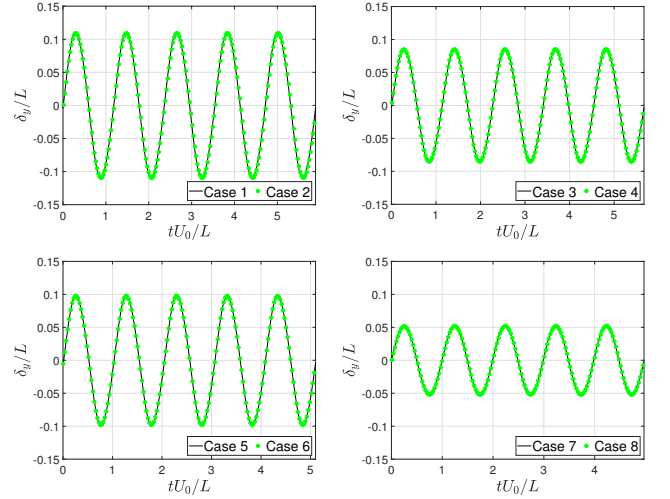


Figure 2: Temporal evolution of the cross-stream displacement of the trailing edge over five cycles corresponding to the eight cases described in Table I.

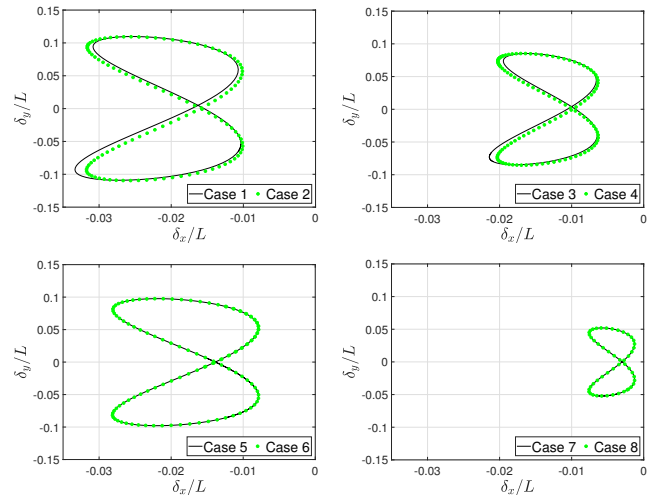


Figure 3: Lissajous curves corresponding to the eight cases described in Table I.

and frequency. Table I further substantiates the similarity between the cases with identical non-dimensional parameters by comparing the mean, maximum and root mean square values of the lift and drag coefficients. Based on these comparisons, we can say that the newly proposed non-dimensional parameters effectively predict the flapping dynamics of multilayered plates. However, even though we observe a good match for the force and transverse flapping dynamics between the cases with identical non-dimensional parameters, the same is not always true for the stream-wise flapping dynamics. Figure 3 presents the Lissajous curves of the trailing edge displacement for each case, and it can be seen that the trailing edge stream-wise displacements do not match for the pairs of cases 1 & 2 and cases 3 & 4 despite these pairs of cases having identical non-dimensional parameters. More specifically, an asymmetric stream-wise displacement of the trailing edge is seen in cases 1 & 3 but not in cases 2 & 4. This asymmetry could be owed to the difference in elastic moduli between the top and bottom layers, which leads to a difference in the degree of bending between the upward and downward cycles, as explained in [26]. The discrepancy between cases having similar non-dimensional parameters can be attributed to the fact that the non-dimensional parameters proposed in this work are based on the Euler-Bernoulli beam equation, which neglects displacements of the beam along its length. These observations indicate a need for one more non-dimensional parameter to completely describe the

flapping dynamics of such multilayered plates, which can be deduced once sufficient investigations into the flapping dynamics of multilayered plates have been carried out.

IV. CONCLUSION

In this work, the non-dimensional parameters that describe the flapping dynamics of multilayered flexible plate in a uniform flow are defined by accommodating the shift in neutral axis of the plate. The defined parameters are validated by utilizing numerical simulations to investigate the flapping dynamics of a two-layered plate placed in a uniform flow. The observations prove the ability of the non-dimensional parameters to describe the cross-stream flapping and force dynamics of multilayered plates to great accuracy. It is also noted that there is still a need for another non-dimensional parameter to ensure similarity in the stream-wise flapping dynamics.

ACKNOWLEDGMENTS

Would like to acknowledge that the work is conducted as part of the SERB-SRG project and usage of the computing facility developed from the OPERA award, BITS–Pilani.

-
- [1] R. Gabbai and H. Benaroya, *J. Sound Vib.* **282**, 575 (2005).
 - [2] D. Bluestein, Y. Alemu, I. Avrahami, M. Gharib, K. Dumont, J. J. Ricotta, and S. Einav, *J. Biomech.* **41**, 1111 (2008).
 - [3] J. Zhang, S. Childress, A. Libchaber, and M. Shelley, *Nature* **408**, 835 (2000).
 - [4] J. J. Allen and A. Smits, *J. Fluids Struct.* **15**, 1 (2001).
 - [5] L. Tang and M. P. Paidoussis, *J. Sound Vib.* **323**, 790 (2009).
 - [6] D. T. Akcabay and Y. L. Young, *Phys. Fluids* **24**, 054106 (2012).
 - [7] D. B. Quinn, G. V. Lauder, and A. J. Smits, *J. Fluid Mech.* **738**, 250 (2014).
 - [8] D. B. Quinn, G. V. Lauder, and A. J. Smits, *Bioinspit. Biomim.* **9** (2014).
 - [9] C. Tang and X. Lu, *Theor. App. Mech. Lett.* **5**, 9 (2015).
 - [10] R.-N. Hua, L. Zhu, and X.-Y. Lu, *Phys. Fluids* **25** (2013).
 - [11] Y. Watanabe, S. Suzuki, M. Sugihara, and Y. Sueoka, *J. Fluids Struct.* **16**, 529 (2002).
 - [12] G. W. Taylor, J. R. Burns, S. M. Kammann, W. B. Powers, and T. R. Welsh, *IEEE J. Oceanic Eng.* **26**, 539 (2001).
 - [13] H. D. Akaydin, N. Elvin, and Y. Andreopoulos, *Exp. Fluids* **49**, 291 (2010).
 - [14] S. Li, J. Yuan, and H. Lipson, *J. Appl. Physics* **109** (2011).
 - [15] D. Kim, J. Cossé, C. Huertas Cerdeira, and M. Gharib, *J. Fluid Mech.* **736**, R1 (2013).
 - [16] P. S. Gurugubelli and R. Jaiman, *J. Fluid Mech.* **781**, 657 (2015).
 - [17] S. Orrego, K. Shoele, A. Ruas, K. Doran, B. Caggiano, R. Mittal, and S. Kang, *App. Energy* **194**, 212 (2017).
 - [18] K. Shoele and R. Mittal, *J. Fluid Mech.* **790**, 582 (2016).
 - [19] M. Piñeirua, O. Doaré, and S. Michelin, *J. Sound Vib.* **346**, 200 (2015).
 - [20] C. Peskin, *Acta Numerica* **11**, 479 (2002).
 - [21] B. S. H. Connell and D. K. P. Yue, *J. Fluid Mech.* **581**, 33 (2007).
 - [22] C. Tang, N.-S. Liu, and X.-Y. Lu, *Phys. Fluids* **27** (2015).
 - [23] T. Bourlet, P. S. Gurugubelli, and R. Jaiman, *J. Fluids Struct.* **54**, 784 (2015).
 - [24] F. B. Tian, H. Luo, L. Zhu, J. C. Liao, and X.-Y. Lu, *J. Comput. Phys.* **230**, 7266 (2011).
 - [25] J. Favier, A. Revell, and A. Pinelli, *J. Fluids Struct.* **53**, 26 (2015).
 - [26] A. K. Saravanakumar, K. Supradeepan, and P. S. Gurugubelli, *Phys. Fluids* **33**, 017108 (2021).
 - [27] M. Shelley, N. Vandenbergh, and J. Zhang, *Phys. Rev. Lett.* **94** (2005).
 - [28] R. K. Jaiman., M. K. Parmar, and P. S. Gurugubelli, *J. Appl. Mech.* **81** (2013).